Macromolecules

Article

pubs.acs.org/Macromolecules

Mechanical Properties of End-Linked PEG/PDMS Hydrogels

Jun Cui, Melissa A. Lackey, Gregory N. Tew,* and Alfred J. Crosby*

Department of Polymer Science and Engineering, University of Massachusetts, Amherst, Amherst, Massachusetts 01003, United States

Supporting Information

ABSTRACT: Poly(ethylene glycol) (PEG)/polydimethylsiloxane (PDMS) hydrogels were synthesized by cross-linking norbornene end-functionalized polymers with a tetrafunctional thiol using thiol−norbornene chemistry. The swelling capacity and mechanical properties, including the Young's modulus (E) and fracture toughness (G_c), of the hydrogels were characterized and quantified as a function of the volume fractions of PEG and PDMS. E and G_c increased simultaneously with the volume fraction of PDMS. The moduli of the hydrogels were quantitatively described and predicted as a function of the volume fraction ratio of PEG to PDMS using the Voigt and Reuss models. The fracture toughness was well described by the Lake−Thomas theory at low volume fractions of PDMS. As the volume fraction of PDMS increased, PDMS not only controlled the swelling capacity of the hydrogels but also contributed to hydrogel toughness.

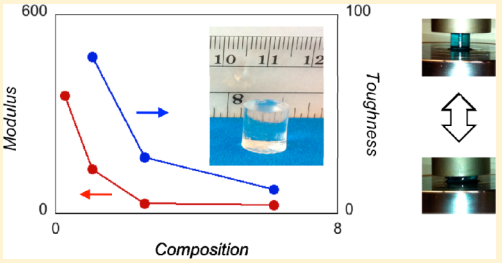

INTRODUCTION

Hydrogels have drawn considerable attention in recent years due to their many potential applications, including use in contact lenses,[1,2] tissue engineering,[3,4] drug delivery,[5] and chemical sensing.[6] Many advantages inherently exist in hydrogels, such as high water content, large deformability compared to metals and ceramics, and environmentally benign components.[7,8] However, most synthetic hydrogels are known to be brittle and fragile, limiting their applications.[8]

Many research groups have focused on improving the mechanical properties of synthetic hydrogels by manipulating the network architecture.[9,10] For example, Okumura and co-workers developed a novel topological gel by introducing sliding cross-linkers into a network, largely improving the extensibility ($\varepsilon_{max} \sim 20$).[11] One of our laboratories synthesized a gel system using a cyclic topology, which simultaneously increased the swelling capacity and Young's modulus, E, of these hydrogels.[12] Gong et al. developed double network (DN) hydrogels composed of one rigid highly cross-linked networks and one loosely cross-linked network.[13] This unique network structure provided high extensibility ($\varepsilon_{max} = 10-20$) and large fracture toughness ($G_c = 100-1000$ J/m^2).[14] Although these novel chemistries have improved the mechanical properties of hydrogels, they require the use of complex architectures, which make them difficult to adopt broadly.

Inspired by the toughening mechanism of filled rubber systems,[15] several research groups have introduced a novel class of hydrogels with simple architectures, where the polymer chains were cross-linked in the presence of particles. The first nanocomposite hydrogel was made by Haraguchi et al., in which clay nanoparticles were dispersed in a poly(N-isopropylacrylamide) network.[16] The resultant hydrogels could be elastically stretched to ∼10 times their original length.[17] Similarly, Creton and co-workers developed a chemically cross-linked hybrid hydrogel that was synthesized by cross-linking N,N-dimethylacrylamide in the presence of silica nanoparticles.[18] Although the addition of the silica nanoparticles had little influence on the water capacity, it improved E and G_c of the hydrogels simultaneously. The values of E ranged from 25 to 170 kPa, and G_c was increased by an order of magnitude to ∼80 J/m^2. The significant increase in mechanical properties was due to the adsorption of the polymer chains to the silica particles.[19] In general, these examples have shown that the incorporation of particles into a polymer network can improve the mechanical properties and that stronger interactions between the particles and the polymer matrix result in a stiffer and tougher hydrogel. However, the interactions between the polymer matrix and the nanoparticles have been limited, so far, to hydrophobic and van der Waals interactions, which are both relatively weak.

Similar to the strategy used in the nanocomposite hydrogels, nano- or microscale polymer domains have also been introduced into a polymer matrix using different chemistries to improve the mechanical properties.[20,21] One method was to take advantage of the phase separation of triblock or multiblock copolymers, leading to physically cross-linked network.[21,22] Many research groups have utilized this method to create gels with well-defined architectures, but the gels usually had weak mechanical properties limited by the physical interactions within the cross-links.[22,23] Another approach to improve gel properties was to attach hydrophobic components into polymer networks. The hydrophobic components aggregated within the hydrophilic polymer matrix, reduced the swelling capacity and improved the mechanical strength of the hydrogels.[24−26]

Received: March 22, 2012
Revised: July 6, 2012
Published: July 20, 2012

dx.doi.org/10.1021/ma300593g | Macromolecules 2012, 45, 6104−6110

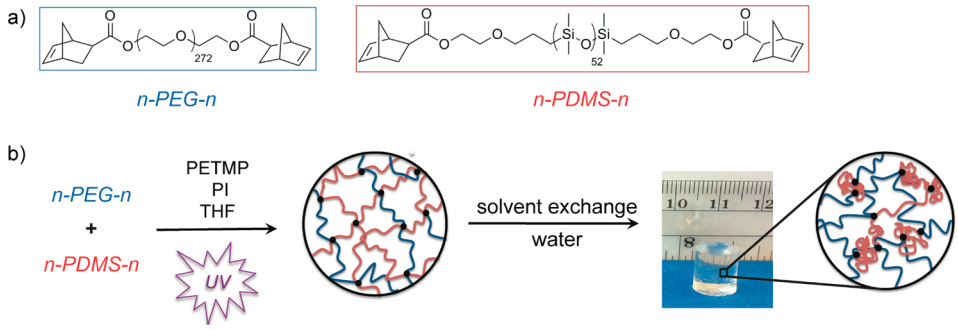

Figure 1. (a) Structures of norbornene end-functionalized poly(ethylene glycol) (n-PEG-n) and polydimethylsiloxane (n-PDMS-n). (b) Synthesis and swelling of the PEG/PDMS hydrogels (PETMP = pentaerythritol tetrakis(3-mercaptopropionate); PI = photoinitiator).

Table 1. Volume Fractions of PEG, PDMS, and Total Polymer in the Preparation and Equilibrium Swollen (Hydrated) States and Equilibrium Swelling Ratios (Q)

		preparation state[a]			hydrated state[b]			
sample	name	$\phi_{PEG,0}$	$\phi_{PDMS,0}$	ϕ_0	ϕ_{PEG}	ϕ_{PDMS}	ϕ	Q
1	$PEG_{100}PDMS_0$	0.084	0	0.084	0.024	0	0.024	38
2	$PEG_{70}PDMS_{30}$	0.069	0.011	0.080	0.040	0.007	0.047	20
3	$PEG_{50}PDMS_{50}$	0.059	0.023	0.082	0.067	0.027	0.093	11
4	$PEG_{30}PDMS_{70}$	0.043	0.041	0.084	0.091	0.088	0.18	5.7
5	$PEG_{10}PDMS_{90}$	0.020	0.072	0.092	0.099	0.36	0.46	2.2

[a]In the preparation state, $\phi_0 = \phi_{PEG,0} + \phi_{PDMS,0}$. [b]In the hydrated state, $\phi = \phi_{PEG} + \phi_{PDMS}$ and $\phi + \phi_{water} = 1$. The subscripts in each sample name show the molar ratio of PEG to PDMS in the preparation state.

Although progress has been made to improve the properties of hydrogels using this strategy, there is no model that adequately describes the influence of the hydrophobic components on the mechanical properties of the hydrogels.

For swollen networks, or gels, with a single polymer component, many classic theories are available to quantitatively correlate their swelling and mechanical properties with the network composition. For example, Hubbell et al. synthesized end-linked poly(ethylene glycol)-*co*-peptide hydrogels using Michael-type addition chemistry and quantified their swelling properties using the Miller−Macosko theory combined with Flory's classical network models.[27] Colby and co-workers derived scaling theories to correlate the swelling ratio and elastic modulus with the molecular weight between cross-links and volume fraction of polymers in the swollen networks based on Flory and Rehner's models.[28] Many research groups have used these scaling theories to describe the mechanical properties of swollen networks with different chemistries.[12,29] However, for gels with multiple components, the correlations between mechanical properties and the network structures have not been well established.

In our previous paper, we introduced a simple network system consisting of two cross-linkable components: one hydrophilic polymer and one hydrophobic polymer.[30] Taking advantage of the incompatibility of these two polymers, a composite hydrogel with hydrophobic domains chemically cross-linked into the hydrophilic polymer matrix was formed, where the hydrophobic polymer aggregated into nano- or microdomains. We employed poly(ethylene glycol) (PEG) and polydimethylsiloxane (PDMS) as the hydrophilic and the hydrophobic polymers, respectively. Both polymers were end-functionalized with norbornene moieties, thus allowing simple, efficient photoinitiated thiol−norbornene cross-linking chemistry to be utilized to form the polymer network. Cross-linking with a tetrafunctional thiol was performed in a good solvent for both polymers, resulting in networks with well-defined architectures, and the subsequent transfer to an aqueous environment led to phase separation of the hydrophilic and hydrophobic components. The hydrophilic PEG acted as the network's matrix, while the hydrophobic PDMS domains decreased the swelling capacity while maintaining high resilience. In this paper, we present the systematic characterization of these novel PEG/PDMS hydrogels, focusing mainly on their mechanical properties, including the modulus and fracture toughness, as a function of the hydrogel composition. The initial polymer volume fraction, ϕ_0, was kept constant for all of the experiments, while the relative initial composition of PEG, $\phi_{PEG,0}$, to PDMS, $\phi_{PDMS,0}$, was varied. By combining scaling theories and the Voigt and Reuss models, the moduli of the hydrogels were quantitatively described as a function of the volume fraction ratio of PEG to PDMS.

EXPERIMENTAL SECTION

Hydrogel Synthesis. The norbornene end-functionalized PEG (n-PEG-n) and PDMS (n-PDMS-n) were synthesized by the Mitsunobu coupling reaction according to the procedures described previously.[30] As shown in Figure 1, the desired amounts of n-PEG-n and n-PDMS-n were dissolved in tetrahydrofuran (THF) to form a clear and transparent solution (see Table 1 for the network compositions). The tetrathiol cross-linker, PETMP, and photoinitiator, Irgacure 2959 (1.0 wt %), were then added to make a precursor solution, which was well mixed and transferred to the desired mold. For all the gels, the molar ratio of the total polymer (n-PEG-n and n-PDMS-n) to the cross-linker was 2 to 1, so the molar ratio of the norbornene to thiol groups was 1 to 1. The precursor solution was exposed to ultraviolet (UV) light with a wavelength of 365 nm for 30 min. The cured gel was removed from the mold and washed with excess THF three times to remove unreacted materials. The resulting gel was immersed in deionized water, which was replaced daily until equilibrium swelling was reached.

Swelling Measurements. The weight of the equilibrium-swollen gels in water, $W_{swollen}$, was determined using an analytical balance. The

dx.doi.org/10.1021/ma300593g | *Macromolecules* 2012, 45, 6104−6110

gels were then placed in a dish, open to ambient laboratory conditions, for 2 days, and then dried under vacuum at room temperature for an additional 2 days. The weight of the samples after the drying process was defined as W_{dry}. The swelling capacity of these hydrogels was quantified by the mass swelling ratio, Q, defined in eq 1.

$$Q = \frac{W_{swollen}}{W_{dry}} \quad (1)$$

The equilibrium water content of these hydrogels, WC, was calculated by the equation $(W_{swollen} - W_{dry})/W_{swollen}$.

Compression Testing. Cylindrical samples were prepared using a modified plastic syringe (6 mL) with an inner diameter of 12.5 mm as a mold. The aspect ratio (diameter to height) of all the samples was kept to be ~0.9. An Instron 4468 instrument with two parallel compression platens and a 1 kN load cell was used for uniaxial compression testing of the hydrogels at a compressive strain rate of 0.2 min^{-1}. Soapy water was applied to the interfaces between the sample and the platens in order to create a frictionless boundary condition. Raw data were recorded as force versus displacement, which were then converted to stress versus strain with respect to the initial sample dimensions. The Young's modulus was determined from the initial slope of the linear portion (up to 10% strain) in the stress–strain curve. True stress was calculated using the compressive force divided by the cross-section area of the compressed sample. The extension ratio was determined by the ratio of the sample height under deformation to the initial height of the sample.

Fracture Measurements. Rectangular hydrogel samples were made using a custom Teflon mold with a length of 3 cm and a width of 3 cm. The samples were cut in half after swelling. An arbitrary notch with a length of 1–2 mm was created on one edge of the sample. The sample was gripped in the Instron 4468 tensile testing instrument with a 50 N load cell. Velcro was used to prevent slipping between the sample and the grips. The measurements were performed at an extension rate of 10 mm/min. Raw data were recorded as force versus displacement, which were then converted to stress versus strain with respect to the initial sample dimensions. Assuming a fixed displacement during crack propagation, the fracture energy was determined by the stored elastic energy, which was the area under the stress–strain curve. Then the critical strain energy release rate, G_c, was calculated by multiplying that area by the initial length of the sample.

RESULTS

Gels with different initial volume fractions of PEG ($\phi_{PEG,0}$) and PDMS ($\phi_{PDMS,0}$) were prepared in THF. The total polymer volume fraction was held constant ($\phi_0 = 0.08–0.09$) (Table 1), while $\phi_{PDMS,0}$ was increased from 0 to 0.072. Fixing ϕ_0 allowed us to neglect the impact of the total polymer volume fraction and to only examine the influence of the ratio of PEG to PDMS, especially in the context of swelling in water.

Swelling Properties. Figure 2 shows the equilibrium swelling ratio, Q, and the equilibrium water content, WC, as a function of $\phi_{PDMS,0}$, where Q decreased from 38 to 2.2 and WC decreased from 97% to 54% as $\phi_{PDMS,0}$ increased from 0 to 0.072. Empirically, Q scaled with $\phi_{PDMS,0}$ as $Q \sim \phi_{PDMS,0}^{-1.18}$ (Supporting Information Figure 1), indicating that the incorporation of the hydrophobic PDMS effectively decreased the water capacity of the hydrogels. This result was different from conventional hydrogels, where the swelling capacity scales with the total polymer volume fraction.[28] In this system, changing ϕ_0 while keeping the ratio of $\phi_{PEG,0}$ to $\phi_{PDMS,0}$ constant had little influence on the swelling capacity of the hydrogels (SI Figure 2). This further suggested that, rather than ϕ_0, the ratio of $\phi_{PEG,0}$ to $\phi_{PDMS,0}$ determined Q in these PEG/PDMS hydrogels. Additionally, the initial volume fraction of the PEG and PDMS controlled the swelling capacity in the hydrophilic phase. Assuming PDMS did not swell in water, the swelling ratio in the PEG phase linearly increased with $\phi_{PDMS,0}$ (SI Figure 9). Thus, the swelling capacity of this PEG/PDMS hydrogel system can be tuned by the ratio of $\phi_{PEG,0}$ to $\phi_{PDMS,0}$.

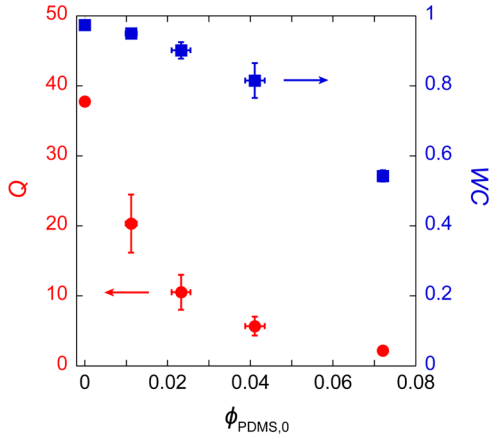

Figure 2. Swelling ratio (Q) and equilibrium water content (WC) as a function of $\phi_{PDMS,0}$. Standard deviations were calculated from at least three samples.

Mechanical Properties. The mechanical properties of these equilibrium swollen PEG/PDMS hydrogels, including the maximum strain (ε_{max}), maximum stress (σ_{max}), and Young's modulus (E), were investigated under compression. Representative curves of true stress as a function of extension ratio and strain for the PEG/PDMS hydrogels with different compositions are shown in Figure 3a. The strain and true stress at the point that permanent failure occurred correspond to ε_{max} and σ_{max}, indicating the compressibility and strength, respectively. These quantities are plotted as a function of $\phi_{PDMS,0}$ in Figure 3b. Interestingly, ε_{max} maintained a constant value of more than 0.8 for $\phi_{PDMS,0} \leq 0.041$, but it significantly decreased when $\phi_{PDMS,0} = 0.072$. In addition, σ_{max} was found to increase initially with $\phi_{PDMS,0}$ and then plateaued for $\phi_{PDMS,0} > 0.023$. Thus, among the hydrogels tested in this study, those with $0.023 \leq \phi_{PDMS,0} \leq 0.041$ had the largest capacity for energy storage in compression ($U = \int \sigma \, d\varepsilon$, where U is the stored energy).

The Young's modulus, E, under compression was determined from the slope of the initial linear portion (up to a strain of 0.1) of the stress–strain curve. As shown in Figure 4, with increasing $\phi_{PDMS,0}$, E also increased by almost 2 orders of magnitude, from 5.6 kPa ($\phi_{PDMS,0} = 0$) to 360 kPa ($\phi_{PDMS,0} = 0.072$). This increase can be attributed to the decrease in water content of the PEG/PDMS hydrogels with increasing $\phi_{PDMS,0}$. However, unlike conventional gels, where $E \sim \phi^{2.25}$ in a good solvent and $E \sim \phi^3$ in a theta solvent,[28] the modulus of the PEG/PDMS hydrogels scaled as $E \sim \phi^{1.33}$ (SI Figure 3). This indicates that the conventional scaling laws are not applicable for the PEG/PDMS hydrogels described here. A model that quantifies E as a function of ϕ_{PDMS} and ϕ_{PEG} is described later in the Discussion section.

Fracture Properties. The fracture properties of the PEG/PDMS hydrogels were measured in terms of the critical strain energy release rate, G_c. The measured values of G_c are plotted as a function of $\phi_{PDMS,0}$ in Figure 5, and it can be seen that G_c increased significantly as $\phi_{PDMS,0}$ increased. For the PEG hydrogel ($\phi_{PDMS,0} = 0$) G_c was 7 J/m^2, a value comparable to conventional hydrogels, such as polyacrylamide (PAAm) gels (G_c = 1–10 J/m^2).[31] As PDMS was incorporated into the hydrogels, G_c increased up to 100 J/m^2. This suggests that the

dx.doi.org/10.1021/ma300593g | Macromolecules 2012, 45, 6104–6110

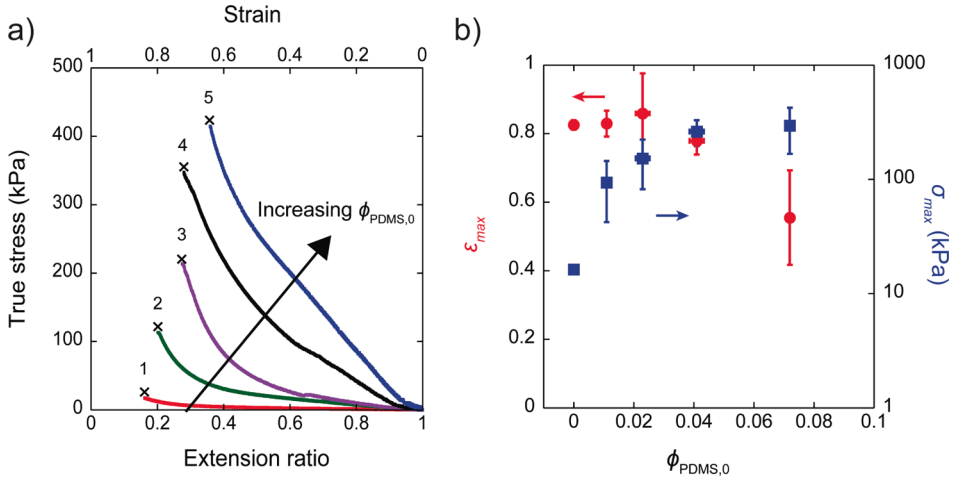

Figure 3. Mechanical properties measured by uniaxial compression testing: (a) representative curves of true stress as a function of extension ratio and strain for the hydrogels with increasing $\phi_{PDMS,0}$ (the details of the compositions are shown in Table 1); (b) the maximum strain (ε_{max}) and maximum true stress (σ_{max}) plotted as a function of $\phi_{PDMS,0}$. Standard deviations were calculated from at least three samples.

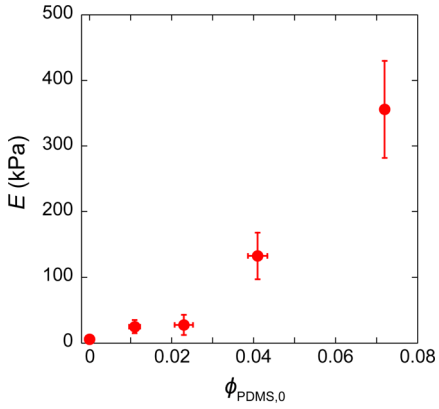

Figure 4. Young's modulus (E) as a function of $\phi_{PDMS,0}$. Standard deviations were calculated from at least three samples.

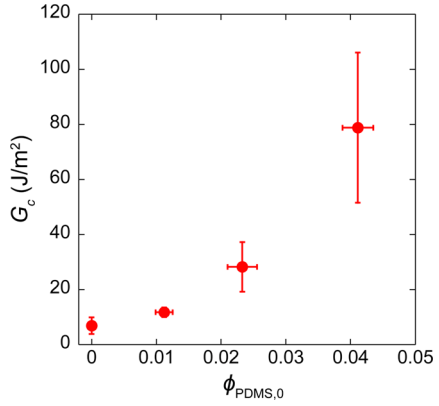

Figure 5. Critical strain energy release rate (G_c) as a function of $\phi_{PDMS,0}$. Standard deviations were calculated from at least three samples.

addition of PDMS effectively toughens the PEG hydrogels by more than 10 times.

DISCUSSION

The mechanical measurements described above indicate that the incorporation of PDMS into the PEG-based network can effectively increase E and G_c simultaneously. Many classic theoretical models are available to correlate the modulus and fracture toughness to the polymer volume fraction, such as the Flory–Rehner theory,[32,33] the affine and phantom network models, etc.;[34] however, most of these models were developed based on swollen networks with a single polymer component. Models that accurately describe the mechanical properties of gels with two polymer components are still undeveloped. In this section, we quantitatively describe how the mechanical properties of the PEG/PDMS gels, including E and G_c, correlate to the volume fractions of the PEG and PDMS.

Young's Modulus. From the network structure aspect, the PEG/PDMS gels acted as swollen networks with nano- or microscale hydrophobic domains. This has some similarities to a rubber matrix filled with rigid particles, the properties of which can be described by the classic Guth–Gold model.[35] In this model, when the volume fraction of the particles, $\phi_{particle}$, is less than 0.1, the composite modulus is related to $\phi_{particle}$ as

$$E = E_0(1 + 2.5\phi_{particle} + 14.1\phi_{particle}^2) \quad (2)$$

where E_0 is the Young's modulus of the polymer matrix. In the PEG/PDMS hydrogel system, ϕ_{PDMS} is defined as $\phi_{particle}$ and E_0 is assumed to be the Young's modulus of the PEG gel at $\phi_{PDMS} = 0$. SI Figure 4 presents the experimental values of E for the PEG/PDMS hydrogels as a function of ϕ_{PDMS}, and compares E with the theoretical prediction from the Guth–Gold model. The experimental E values were significantly larger than the predicted values. The difference was believed to result from two underlying reasons. First, the model was developed to describe systems with weak interactions between the particles and the matrix, so it did not account for the strong covalent interactions between the PDMS domains and the PEG-based network. Being covalently bonded to the matrix, the PDMS domains acted as additional cross-linking points that stiffened the hydrogels. Thus, the equation underestimated the effect of the PDMS domains on E of the hydrogels. Second, the model assumed that E_0 of the polymer matrix was not affected by the addition of the particles. However, in these PEG/PDMS hydrogels, since as $\phi_{PDMS,0}$ increased, Q significantly decreased (Figure 2), E of the PEG-based matrix was expected to change with $\phi_{PDMS,0}$, according to the conventional scaling law $E \sim Q^{-2.25}$.[28] As a result, the difference in the experimental data and the Guth–Gold model prediction demonstrates that this PEG/

dx.doi.org/10.1021/ma300593g | Macromolecules 2012, 45, 6104–6110

PDMS hydrogel system is fundamentally different from the filled hydrogels, where the particles and matrix have weaker interactions and the addition of particles has little influence on the swelling properties.[18] Thus, a model that includes the contributions of both the hydrophobic PDMS domains and the hydrophilic PEG matrix is required.

To better capture the variation in modulus, the hydrogel can be described as two interconnected phases: one water-swollen PEG phase and one hydrophobic PDMS phase, with volume fractions $\phi_{PEG} + \phi_{water}$ and ϕ_{PDMS}, respectively, where $\phi_{PEG} + \phi_{water} + \phi_{PDMS} = 1$. This assumed that water only swelled the PEG phase. The Voigt and Reuss models[36] were employed to analyze E of the hydrogels. These models were developed to describe E of composites with two components in different arrangements, providing the upper and lower limits of E for the composites. Equations 3a and 3b represent E as described by the Voigt and Reuss models, respectively, where κ is defined as $\phi_{PEG,0}/\phi_{PDMS,0}$ ($\approx \phi_{PEG}/\phi_{PDMS}$, assuming the conversions of the thiol−norbornene chemistry for the PEG and PDMS were identical), so that $E_{hydrogel}$ was dependent upon the initial volume fractions of the gels' components (see eqs S1−S8 for details).

Voigt:

$$E_{hydrogel} = \phi_{PDMS}\left[E_{PEG,0}\kappa^{2.25}\left(\frac{1}{1-\phi_{PDMS}} - 1\right)^{1.25} + E_{PDMS,0}\right] \quad (3a)$$

Reuss:

$$\frac{1}{E_{hydrogel}} = \phi_{PDMS}\left[\frac{(\phi_{PDMS}{}^{-1} - 1)^{3.25}}{E_{PEG,0}\kappa^{2.25}} + \frac{1}{E_{PDMS,0}}\right] \quad (3b)$$

The modulus of the PDMS phase, E_{PDMS}, was assumed to be E of dry PDMS synthesized via the same cross-linking chemistry, $E_{PDMS,0}$, which was measured using compression testing, while the modulus of the swollen PEG phase was determined by the scaling law,[28] as shown in eq 4. In this equation, $E_{PEG,0}$ was the modulus of PEG when the volume fraction of PEG was equal to one. This value was calculated based on the scaling theory, $E_{PEG,0} \approx E_{PEG}\phi^{-2.25}$, where E_{PEG} was the modulus of equilibrium-swollen PEG when $\phi_{PDMS} = 0$ and $\phi_{PEG} = 0.024$ (Table 1).

$$E_{PEG} \approx E_{PEG,0}(\phi_{PEG}/(\phi_{PEG} + \phi_{water}))^{2.25} = E_{PEG,0}(\kappa/(\phi_{PDMS}{}^{-1}))^{2.25} \quad (4)$$

To simplify this equation, ϕ_{PDMS} was empirically correlated to κ, as $\phi_{PDMS} \approx 0.078\kappa^{-1.28}$ (SI Figure 5). After substituting this relationship into eq 3, $E_{hydrogel}$ is described by κ as shown in Figure 6, which plots theoretical curves of E as a function of κ predicted by the Voigt (eq 3a) and Reuss (eq 3b) models as well as the experimental values. The good fit to the experimental data indicates that the composite models are able to quantitatively describe the moduli of these hydrogels.

Theoretically, the Voigt and Reuss models provide the upper and lower limits of E of composites, respectively.[36] In the PEG/PDMS hydrogels, the difference between the two limits

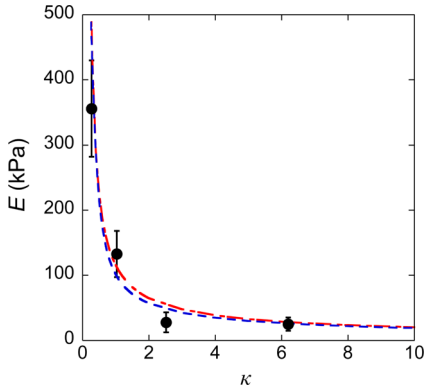

Figure 6. Young's modulus (E) as a function of κ ($= \phi_{PEG,0}/\phi_{PDMS,0}$) (black circles) for the PEG/PDMS hydrogels. Standard deviations were calculated from at least three samples. Red and blue dashed lines represent the theoretical values of E as predicted by the Voigt and Reuss models for the hydrogels, respectively.

provided by the Voigt and Reuss models was rather small. This difference was dependent upon E of each component in the composite, where a large difference in E would lead to a significant difference between the two limits. In this PEG/PDMS hydrogel system, E of the PDMS phase was comparable with E of the hydrated PEG phase such that the influence of the arrangement of the two phases is negligible (SI Figures 6 and 7). Therefore, both of the composite models described above were able to quantify the moduli of the PEG/PDMS hydrogels as a function of the ratio of the initial volume fractions of PEG to PDMS.

Fracture Toughness. The Lake−Thomas theory has been used to describe the fracture toughness of polymer networks as $G_c = NUf$, where N is the degree of polymerization, U is the bond dissociation energy, and f is the areal chain density.[37] For swollen polymer networks, $f = \phi/a^2N^{1/2}$, where a is the monomer size, derived by the scaling theory,[38] so that

$$G_c = \frac{N^{1/2}U}{a^2}\phi \quad (5)$$

where G_c is proportional to the volume fraction of the polymer (ϕ). For the PEG hydrogel ($\phi_{PDMS,0} = 0$), the theoretical G_c value calculated using eq 5 (5.3 J/m^2) was comparable to the value that was determined by the fracture toughness measurement (6.9 J/m^2). However, for the PEG/PDMS hydrogels, a stronger dependence of G_c upon ϕ was observed, where G_c scaled with the volume fraction of the total polymer by 1.21 (SI Figure 8).

Again considering the PEG/PDMS gel as two phases (one swollen PEG phase and one PDMS phase), as can be seen in Table 1, the swollen PEG phase is the major component at small $\phi_{PDMS,0}$. Assuming the crack only propagated through the major PEG phase, the experimental G_c values are plotted as a function of the volume fraction of PEG in the PEG phase, $\phi_{PEG/water}$, along with the theoretical G_c values for the PEG phase according to eq 5. As shown in Figure 7, for the gels with small $\phi_{PEG/water}$, the experimental values were comparable with the Lake−Thomas theory's prediction. This indicated that fracture toughness of the gels was predominantly determined by the swollen PEG phase. On the other hand, at large $\phi_{PEG/water}$, the experimental values were significantly higher than the prediction. Since $\phi_{PEG/water}$ increased with $\phi_{PDMS,0}$ (SI Figure 9), it is likely that the PDMS phase played an important

dx.doi.org/10.1021/ma300593g | Macromolecules 2012, 45, 6104−6110

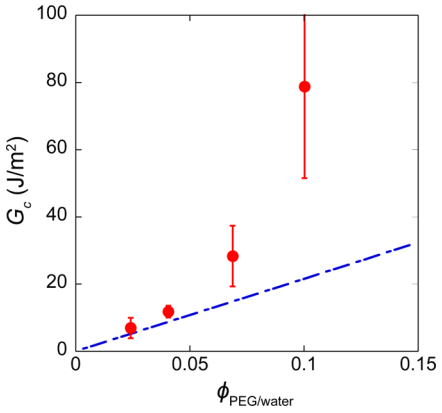

Figure 7. Fracture toughness (G_c) plotted as a function of the volume fraction of PEG in the PEG phase ($\phi_{PEG/water}$). Red dots are the experimental values, corresponding to samples 1 to 4 from left to right; blue line represents the theoretical values calculated using Lake–Thomas theory.

role in the fracture toughness of the gels. For gels with large $\phi_{PDMS,0}$, assuming the crack propagated through the PDMS phase, the theoretical G_c value was calculated based on the material properties of the PDMS according to eq 5, which gave a G_c of 22 J/m^2. This value was also significantly lower than the experimental values at large $\phi_{PDMS,0}$. This underestimation of the G_c values can be attributed to two possibilities. First, the Lake–Thomas theory that was applied to describe the fracture energy of the PEG/PDMS hydrogels was limited to one phase and did not account for the combination of the strain energy stored in both the PEG and the PDMS phases. Second, the strain energy stored in the PEG/PDMS hydrogels could be nonlinearly coupled with crack propagation processes in this multiphase system, which has also not been considered. More network structure information is required to develop models that could better describe the fracture toughness of these hydrogels, and these investigations are ongoing.

CONCLUSION

In summary, end-linked PEG/PDMS hydrogels were successfully synthesized using simple, efficient thiol–norbornene chemistry, and the swelling and mechanical properties were systematically characterized. By manipulating the volume fractions of the PEG and PDMS, a large range of water content (54%–97%) was achieved. The Young's modulus (E) was significantly improved by increasing the volume fraction of PDMS in the hydrogel, and the relationship between them was quantitatively described by the Voigt and Reuss models. Furthermore, increasing the volume fraction of the PDMS led to tougher hydrogels with G_c up to 100 J/m^2. This simple hydrogel system with enhanced mechanical properties will be a good candidate for many applications, including in the biomedical field and in the design of protective wear. The structure–property relationships developed in this system will provide useful information for the future design of swollen networks.

ASSOCIATED CONTENT

Supporting Information

Details of materials and descriptions of the Voigt and Reuss models as well as supplementary figures. This material is available free of charge via the Internet at http://pubs.acs.org.

AUTHOR INFORMATION

Corresponding Author

*E-mail crosby@mail.pse.umass.edu, Tel 413-577-1313, Fax 413-545-0082 (A.J.C.); e-mail tew@mail.pse.umass.edu, Tel 413-577-1612, Fax 413-545-2873 (G.N.T.).

Notes

The authors declare no competing financial interest.

ACKNOWLEDGMENTS

We acknowledge NSF PIRE (NSF-0730243), DMR-0820506, and CMMI-0531171 for funding. Partial support was provided from ARO W911NF-09-1-0373 and ONR N00014-10-1-0348. This work utilized facilities supported in part by the National Science Foundation under Agreement DMR-0944772. We thank Ms. Katie Gibney and Mr. Hitesh Thaker for their assistance in preparing the manuscript.

REFERENCES

(1) Ellis, E. J.; Salamone, J. C. U.S. Patent 4,151,508, May 1, 1979.
(2) Wichterle, O.; Lim, D. *Nature* **1960**, *185*, 117–118.
(3) Brandl, F.; Sommer, F.; Goepferich, A. *Biomaterials* **2007**, *28*, 134–146.
(4) Lee, K. Y.; Mooney, D. J. *Chem. Rev.* **2001**, *101*, 1869–1879.
(5) Hoare, T. R.; Kohane, D. S. *Polymer* **2008**, *49*, 1993–2007.
(6) Holtz, J. H.; Asher, S. A. *Nature* **1997**, *389*, 829–832.
(7) Wang, Q.; Mynar, J. L.; Yoshida, M.; Lee, E.; Lee, M.; Okuro, K.; Kinbara, K.; Aida, T. *Nature* **2010**, *463*, 339–343.
(8) Calvert, P. *Adv. Mater.* **2009**, *21*, 743–756.
(9) Johnson, J. A.; Turro, N. J.; Koberstein, J. T.; Mark, J. E. *Prog. Polym. Sci.* **2010**, *35*, 332–337.
(10) Tanaka, Y.; Gong, J. P.; Osada, Y. *Prog. Polym. Sci.* **2005**, *30*, 1–9.
(11) Okumura, Y.; Ito, K. *Adv. Mater.* **2001**, *13*, 485–487.
(12) Zhang, K.; Lackey, M. A.; Cui, J.; Tew, G. N. *J. Am. Chem. Soc.* **2011**, *133*, 4140–4148.
(13) Gong, J. P.; Katsuyama, Y.; Kurokawa, T.; Osada, Y. *Adv. Mater.* **2003**, *15*, 1155–1158.
(14) Tanaka, Y.; Kuwabara, R.; Na, Y. H.; Kurokawa, T.; Gong, J. P.; Osada, Y. *J. Phys. Chem. B* **2005**, *109*, 11559–11562.
(15) Gent, A. N. *Engineering with Rubber: How to Design Rubber Components*, 2nd ed.; Hanser: Cincinnati, 2001.
(16) Haraguchi, K.; Farnworth, R.; Ohbayashi, A.; Takehisa, T. *Macromolecules* **2003**, *36*, 5732–5741.
(17) Gong, J. P. *Soft Matter* **2010**, *6*, 2583–2590.
(18) Lin, W. C.; Fan, W.; Marcellan, A.; Hourdet, D.; Creton, C. *Macromolecules* **2010**, *43*, 2554–2563.
(19) Lin, W. C.; Marcellan, A.; Hourdet, D.; Creton, C. *Soft Matter* **2011**, *7*, 6578–6582.
(20) Patrickios, C. S.; Georgiou, T. K. *Curr. Opin. Colloid Interface Sci.* **2003**, *8*, 76–85.
(21) Xiao, L. X.; Liu, C.; Zhu, J. H.; Pochan, D. J.; Jia, X. Q. *Soft Matter* **2010**, *6*, 5293–5297.
(22) Sanabria-DeLong, N.; Agrawal, S. K.; Bhatia, S. R.; Tew, G. N. *Macromolecules* **2007**, *40*, 7864–7873.
(23) Seitz, M. E.; Martina, D.; Baumberger, T.; Krishnan, V. R.; Hui, C. Y.; Shull, K. R. *Soft Matter* **2009**, *5*, 447–456.
(24) Erdodi, G.; Kennedy, J. P. *J. Polym. Sci., Part A: Polym. Chem.* **2005**, *43*, 4965–4971.
(25) Xu, J. Q.; Bohnsack, D. A.; Mackay, M. E.; Wooley, K. L. *J. Am. Chem. Soc.* **2007**, *129*, 506–507.
(26) Abdurrahmanoglu, S.; Can, V.; Okay, O. *Polymer* **2009**, *50*, 5449–5455.
(27) Lutolf, M. P.; Hubbell, J. A. *Biomacromolecules* **2003**, *4*, 713–722.
(28) Obukhov, S. P.; Rubinstein, M.; Colby, R. H. *Macromolecules* **1994**, *27*, 3191–3198.

(29) Malkoch, M.; Vestberg, R.; Gupta, N.; Mespouille, L.; Dubois, P.; Mason, A. F.; Hedrick, J. L.; Liao, Q.; Frank, C. W.; Kingsbury, K.; Hawker, C. J. *Chem. Commun.* **2006**, 2774−2776.
(30) Cui, J.; Lackey, M. A.; Madkour, A. E.; Saffer, E. M.; Griffin, D. M.; Bhatia, S. R.; Crosby, A. J.; Tew, G. N. *Biomacromolecules* **2012**, *13*, 584−588.
(31) Tanaka, Y.; Fukao, K.; Miyamoto, Y. *Eur. Phys. J. E* **2000**, *3*, 395−401.
(32) Flory, P. J.; Rehner, J. *J. Chem. Phys.* **1943**, *11*, 512−520.
(33) Flory, P. J.; Rehner, J. *J. Chem. Phys.* **1943**, *11*, 521−526.
(34) Rubinstein, M.; Colby, R. H. *Polymer Physics*; Oxford University Press: New York, 2003.
(35) Guth, E. *J. Appl. Phys.* **1945**, *16*, 20−25.
(36) Young, R. J.; Lovell, P. A. *Introduction to Polymers*, 2nd ed.; Chapman & Hall: New York, 1991.
(37) Lake, G. J.; Thomas, A. G. *Proc. R. Soc. A* **1967**, *300*, 108−119.
(38) Kundu, S.; Crosby, A. J. *Soft Matter* **2009**, *5*, 3963−3968.